The Permian-Triassic Boundary in the Carnic Alps of Austria (Gartnerkofel Region)			Editors: W.T. Holser & H.P. Schönlaub	
Abh. Geol. B.-A.	ISSN 0378-0864 ISBN 3-900312-74-5	Band **45**	S. 149–163	Wien, Mai 1991

The Permian-Triassic of the Gartnerkofel-1 Core (Carnic Alps, Austria): Carbon and Oxygen Isotope Variation

By MORDECKAI MAGARITZ & WILLIAM T. HOLSER*)

With 13 Text-Figures and 3 Tables

Carinthia
Carnic Alps
Permian/Triassic Boundary
Mass Extinction
Events
Carbon Isotopes
Oxygen Isotopes

Österreichische Karte 1 : 50.000
Blatt 198

Contents

Zusammenfassung

Das detaillierte Kohlenstoff-Isotopenprofil in der Forschungsbohrung Gartnerkofel-1 spiegelt einen komplexen Wechsel im marinen Kohlenstoffzyklus an der Perm/Trias-Grenze wieder. Die Feinheit der Isotopendaten, die Konsistenz über vertikale Fazieswechsel hinweg und die Parallelität zu dem 500 m entfernten Obertagsprofil in der Reppwand zeigen, daß der Kurvenverlauf der Kohlenstoffisotope und Sauerstoffisotope primäre Ursachen haben muß. Am Endpunkt des Kerns, in der Mitte der oberpermischen Bellerophon-Formation, gleichen die hohen $\delta^{13}C$-Werte von über +3 ‰ den Werten, die in anderen Gebieten aus gleich alten Schichten bekannt sind. Etwa 60 m unter der Perm/Trias-Grenze nimmt $\delta^{13}C$ ab. Diese Abnahme verstärkt sich an der P/Tr-Grenze und bildet in der tieferen Werfen-Formation eine komplexe Kurve mit $\delta^{13}C$-Werten von weniger als −1 ‰. In diesem Bereich sind über eine Strecke von 50 m drei Minima ausgebildet, die bisher in andern Gebieten nicht bekannt waren. Dieses Ergebnis weist auf die vollständige, im Vergleich zu den übrigen bisher untersuchten Profilen mächtigere Schichtfolge in der Untertrias des Gartnerkofels hin. Im höheren Teil der Werfen-Formation bleibt $\delta^{13}C$ relativ konstant und beträgt durchschnittlich +1 ‰.

Das Kohlenstoff-Isotopenprofil zeigt an, daß die weltweit hohe Speicherung von organischem Kohlenstoff, die verantwortlich ist für die hohen jungpaläozoischen $\delta^{13}C$-Werte, im Verlauf eines komplexen Oxidationsprozesses verbraucht wurde. Dieser Prozeß setzte schon vor der Perm/Trias-Grenze ein, verstärkte sich aber an der Grenze und setzte sich anschließend in drei Oszillationen fort, bevor er sich noch in der älteren Trias wieder auf Normalwerte einpendelte.

*) Authors' addresses: Dr. MORDECKAI MAGARITZ, Environmental Science and Energy Research, The Weizmann Institute of Science, 76100 Rehovot, Israel; Prof. Dr. WILLIAM T. HOLSER, Department of Geological Sciences, University of Oregon, Eugene, OR 97403, USA.

Das Sauerstoff-Isotopenprofil hat an einer Störung im Triasabschnitt des Profils einen größeren negativen Ausschlag. Die Ursache dafür liegt unseres Erachtens im meteorischen Wasseraustausch in der Störungsbrekzie. Die Tatsache, daß der Kurvenverlauf nur in der unmittelbaren Nachbarschaft der Störung abweicht, beweist, daß das restlich Profil kaum spätere Veränderungen erlitten hat. Das Hauptkennzeichen des Sauerstoff-Isotopenprofils ist eine Abnahme von rund −3 ‰ im oberen Teil der Bellerophon-Formation unter der Perm/Trias-Grenze. Dieser Kurvenverlauf kann entweder als Temperaturzunahme oder als Abnahme des Grades der Evaporation des Meeres zu dieser Zeit gedeutet werden. Dafür finden sich jedoch im Sediment kaum Hinweise, weshalb die eigentliche Ursache für die Änderung beider Kurven weiterhin unklar bleibt.

Abstract

A detailed profile of carbon isotopes in the Gartnerkofel core indicates the complexity of changes in the marine carbon cycle near the P/Tr boundary. The fine detail in the isotope record, its consistency among sedimentary facies, and its equivalence with an outcrop section 500 m away, indicate that all of the carbon isotope record and most of the oxygen isotope record are essentially primary. At the bottom of the core, in the middle of the Bellerophon Formation, high $\delta^{13}C$ values of over +3 ‰ approach those recorded elsewhere for the Late Permian. A decrease of $\delta^{13}C$ begins about 60 m below the P/Tr boundary, and this drop accelerates smoothly through the boundary to a complex zone of less than −1 ‰ in the lower Werfen Formation. In this zone three minima are spread over an interval of about 50 m, an aspect not found in any other sections so far analyzed, suggesting that the Gartnerkofel section is more complete. At higher levels in the Werfen Formation, $\delta^{13}C$ remains relatively constant at slightly above +1 ‰. The profile indicates that the worldwide high storage of organic carbon believed to be responsible for the Late Paleozoic high of $\delta^{13}C$, was substantially consumed in a complex oxidation that began substantially before the P/Tr boundary, progressed smoothly through the boundary, and suffered a succession of three excursions, before settling into a more normal phase later in the Early Triassic.

The oxygen isotope profile undergoes a major negative excursion around a fault in the Triassic section. This is expected as a result of exchange with meteroic water circulation in a fault breccia, but the fact that this excursion is limited to the immediate vicinity of the fault suggests that the rest of the section has suffered little of such alteration. The major primary feature displayed in the oxygen profile is a drop of about −3 ‰ in the upper part of the Bellerophon Formation, below the P/Tr boundary. The drop can be interpreted as a rise in temperature or alternatively as a decrease in degree of evaporation of the sea. However, the magnitude of either change would be greater than expected from the sedimentary record, so the interpretation of this change remains open.

1. Introduction

The ratio of stable carbon isotopes in marine carbonates, $^{13}C/^{12}C$, usually expressed as a differential "del value", $\delta^{13}C$ in ‰, depends primarily on the relative net production (higher, positive $\delta^{13}C$) or consumption (lower, negative $\delta^{13}C$) of organic carbon in the global cycle. As a measure of the direction the carbon cycle is working at any particular geological time, it has considerable potential for monitoring and understanding mass extinction events, insofar as these events may involve the carbon cycle as a whole: as changes in productivity, storage and erosion of organic carbon on a worldwide scale (W.T. HOLSER et al., 1986; M. MAGARITZ, 1989). Profiles of $\delta^{13}C$ in marine carbonates show a rather sudden decrease in connection with other extinction events: the Precambrian/Cambrian (M. MAGARITZ et al., 1986), Ordovician/Silurian (C.J. ORTH et al., 1986), Frasnian/Famennian (P.E. PLAYFORD et al., 1984), Devonian/Carboniferous (D. XU et al., 1986), Cenomanian/Turonian (E.G. KAUFFMAN et al., 1988) and Cretaceous/Tertiary (K/T) (S.V. MARGOLIS et al., 1987).

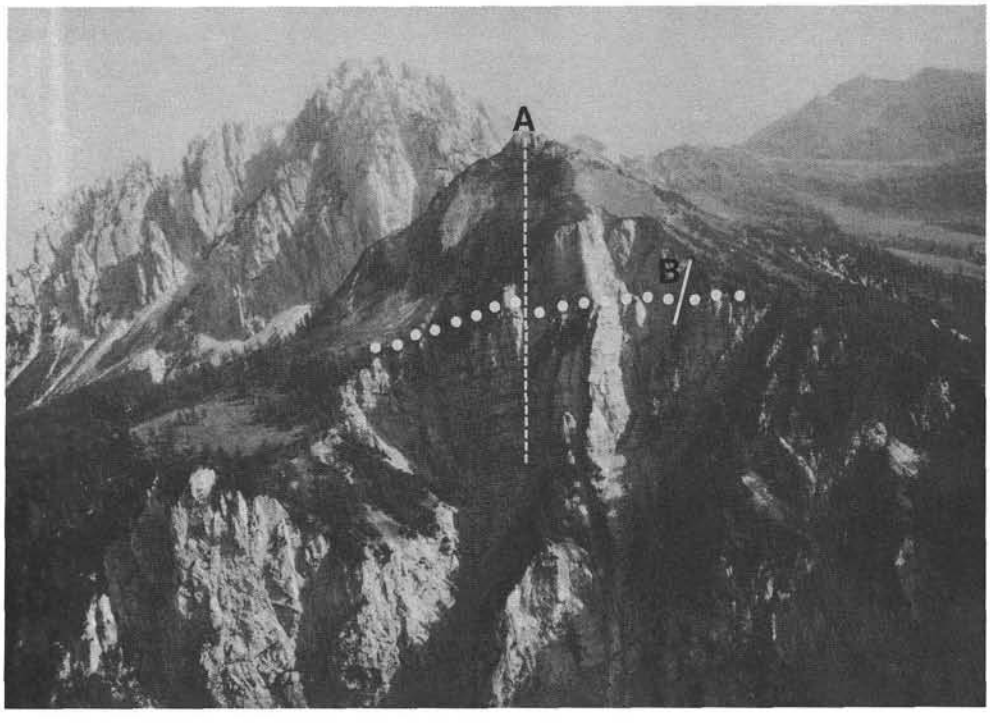

Text-Fig. 1.
Aerial photograph from the north of the Reppwand with the Gartnerkofel (2195 m) in the background.
A: Drill site on Kammleiten (1998 m);
B: Top of the outcrop section.
Dotted line indicates the Permian–Triassic boundary between the Bellerophon Formation (below) and the Werfen Formation above.
Photo: G. FLAJS, Aachen.

Near the Permian/Triassic (P/Tr) boundary, we have demonstrated a very large drop in $\delta^{13}C$ (W. T. HOLSER et al., 1986a) from the relatively high values that characterized late Paleozoic time (B.N. POPP et al., 1986). The drop has been found in many classical sections of the P/Tr boundary throughout Tethys (A. BAUD et al., 1989), and in particular in the Dolomite Alps west of GK-1 (M. MAGARITZ et al., 1988). In a reconnaissance of outcrops in the Gartnerkofel area (Text-Fig. 1), we found a similar drop in the profile of $\delta^{13}C$ (W.T. HOLSER & M. MAGARITZ, 1985). Consequently, a detailed study of carbon isotope variations was one of the principal objectives of this research project.

Carbon isotope ratios in the organic carbon component of the core are now under study, and the results will be published at a later date.

2. Methods

Samples for analysis were for the most part obtained as a split of powder prepared from the billet remaining after thin section preparation. Thus the samples analyzed for carbon and oxygen isotope are strictly correlative with those analyzed chemically and studied in thin section.

CO_2 for mass spectrometric analysis was recovered by reacting the dolomite with 95 % phosphoric acid (1.80 specific gravity) at 25°C (J.M. MCCREA, 1950). Only part of the CO_2 generated, that from the fourth to at least the forty-eighth hour, was collected for carbon and oxygen isotope analysis of the dolomite (R.N. CLAYTON et al., 1968). Variation of $\delta^{18}O$ has been found by WALTERS et al. (1972) in fractionated extraction of CO_2 from solid carbonate. In dolomite samples the first fraction (0–4 hr.) may contain 5–10 % of CO_2 derived from the dolomite. If this is omitted, it will cause deviations of no more thant 0.2 ‰ in the results. The CO_2 was analyzed with a Varian 250 mass spectrometer. The results are expressed in the conventional "δ" per mil notation relative to the PDB standard. Isotope values were calibrated using NBS-19 calcite standard ($\delta^{18}O$ = −2.20 ‰, $\delta^{13}C$ = +1.96 ‰). Reproducibility of duplicate samples is better than 0.1 ‰ for $\delta^{13}C$ and 0.15 ‰ for $\delta^{18}O$.

3. Results

The analytical results are tabulated in Tables 1 and 2. The general result (Table 1) is an accelerating downward trend of $\delta^{13}C$, continuing through the Tesero Horizon and the P/Tr boundary, to a complex minimum in the lower part of the Werfen Formation followed by a generally constant level of $\delta^{13}C$ in the upper part of the Werfen Formation (Text-Fig. 2). Oxygen isotope ratios are less consistent: in some intervals approximately correlated with $\delta^{13}C$, but not generally correlated. These results are considered below by dividing the core section into 4 units based on the sedimentology, some of which were further subdivided (Text-Fig. 2). Unit 1, the (Permian) Bellerophon Formation was divided into two parts based on the carbon isotope data. The upper part (Unit 1B) begins with a gradual drop of $\delta^{13}C$.

Table 1.
Oxygen and carbon isotope analysis of carbonates from core Gartnerkofel-1.

Sample No.	Depth [m]	$\delta^{18}O$	$\delta^{13}C$	Sample No.	Depth [m]	$\delta^{18}O$	$\delta^{13}C$	Sample No.	Depth [m]	$\delta^{18}O$	$\delta^{13}C$
1	57.53	-1.40	0.98	27	95.17	-4.60	1.32	54	127.46	-4.93	1.21
2	58.81	-3.79	1.46	28	95.30	-4.49	1.35	55	127.55	-4.83	1.14
3	60.88	-2.64	1.07	29	95.90	-4.69	1.35	56	130.10	-5.25	1.23
4	61.65	-3.06	1.17	30	96.05	-4.79	1.31	57	130.40	-5.46	1.13
5	63.00	-4.62	1.45	31	97.40	-3.58	1.48	58	130.55	-5.47	1.14
6	64.95	-3.88	1.44	32	99.46	-5.15	1.16	59	134.53	-3.43	1.39
7	65.70	-2.82	1.08	33	100.42	-4.00	1.29	60	136.50	-2.94	1.55
8	70.62	-4.81	1.58	35	102.93	-5.23	0.90	61	137.23	-2.63	1.64
9	71.70	-4.27	1.71	36	103.45	-2.06	1.27	63	138.96	-2.51	1.63
10	72.10	-4.20	1.54	37	103.78	-4.28	1.15	64	140.60	-3.87	1.29
11	73.75	-3.90	1.55	38	105.32	-3.38	1.27	65	141.54	-3.04	1.56
12	74.40	-3.60	1.70	39	105.90	-2.46	1.13	66	142.74	-3.32	1.55
13	75.32	-3.20	1.72	40	107.75	-5.38	1.28	67	143.26	-3.62	1.58
14	75.90	-4.23	1.66	41	110.02	-4.87	1.28	68	144.33	-3.19	1.55
15	76.30	-4.08	1.59	42	111.42	-4.65	1.26	69	146.08	-3.48	1.37
17	79.67	-4.57	1.19	43	112.43	-5.04	1.32	70	146.66	-3.76	1.31
18	81.52	-4.48	1.51	44	113.20	-4.43	1.35	71	147.60	-3.65	1.36
19	82.60	-4.26	1.48	44a	113.30	-4.19	1.40	72	149.34	-4.97	1.08
20	82.85	-4.83	1.36	45	114.00	-4.17	1.35	73	149.61	-4.18	1.27
21	84.37	-4.95	1.31	46	115.95	-4.76	1.25	74	152.57	-4.78	1.24
22	86.26	-4.70	1.53	47	117.70	-4.44	1.33	75	152.69	-4.23	1.15
23	86.92	-4.70	1.30	49	119.27	-4.44	1.35	76	152.75	-4.08	1.32
24	88.85	-4.61	1.32	50	123.50	-5.12	1.30	77	153.50	-4.95	1.06
25	90.30	-4.05	1.49	52	127.04	-5.07	1.22	78	154.11	-4.57	1.13
26	90.56	-4.46	1.43	53	127.30	-5.16	1.20	79	158.33	-3.83	1.35

Table 1 (continued).

Sample No.	Depth [m]	$\delta^{18}O$	$\delta^{13}C$	Sample No.	Depth [m]	$\delta^{18}O$	$\delta^{13}C$	Sample No.	Depth [m]	$\delta^{18}O$	$\delta^{13}C$
80	161.04	-4.04	1.35	136	189.30	-4.86	0.47		209.64	-4.53	0.48
81	162.36	-4.27	1.31	137	189.65	-4.25	0.24		209.80	-4.85	0.39
81b	163.50	-6.43	1.02	138	189.80	-4.37	0.21		210.00	-7.28	0.30
82	163.88	-5.06	1.18	139	190.00	-4.17	0.02	172	210.03	-9.08	0.26
83	164.32	-4.28	1.18	140	190.21	-2.98	-0.30		210.50	-4.93	0.42
84	164.60	-4.51	1.17	141	190.50	-2.58	-0.35		210.90	-6.82	0.24
85	166.35	-3.62	1.24	142	190.66	-2.69	-0.27		211.25	-5.24	-0.01
86	167.98	-4.74	1.23	144	191.06	-3.28	-0.05	173	211.33	-5.41	-0.07
87	168.78	-3.63	1.37	145	191.53	-2.68	-0.41		211.70	-4.24	-0.05
88	169.10	-3.66	1.45	146	192.23	-2.59	-0.41	175	211.85	-4.41	-0.04
89	171.33	-4.20	1.12	147	192.90	-2.33	-0.62		212.00	-3.55	-0.19
90	173.53	-4.00	1.17	148	193.00	-2.25	-0.67	176	212.20	-3.46	-0.25
93	175.10	-4.08	0.81	149	193.55	-2.44	-0.51	177	212.30	-3.73	-0.32
94	176.37	-4.58	0.97	150	193.80	-3.04	-0.42	178	213.50	-3.78	-1.03
95	177.43	-5.06	0.93	151	194.33	-2.73	-0.30	179	213.65	-4.00	-0.97
96	177.72	-5.23	0.82	152	194.75	-2.68	0.35	180	214.05	-3.76	-1.14
97	179.64	-3.55	0.46	153	195.15	-2.38	-0.02	181	214.25	-3.82	-1.14
98	180.33	-4.89	0.31	154	195.38	-2.48	-0.11	182	215.07	-5.14	-1.41
99	181.37	-3.16	0.14	155	195.90	-2.33	-0.23	183	215.35	-3.68	-1.28
100	181.57	-4.04	0.01	156	196.23	-2.87	0.08	184	215.70	-7.44	-0.93
102	182.00	-4.68	-0.32	158	197.05	-3.03	0.10	186	216.52	-4.96	-1.12
103	182.20	-3.89	-0.25	159	197.73	-2.98	0.10	187	219.70	-4.44	-1.15
104a	182.70	-3.94	-0.56	160	198.36	-2.57	-0.02	188	220.10	-4.55	-1.39
104b	183.28	-4.66	-0.79	161	198.70	-2.98	-0.03	189	220.20	-4.46	-1.57
105	183.40	-4.34	-0.67	162	199.15	-3.78	0.55	190	220.35	-6.51	-1.50
106	183.51	-4.84	-0.70	163	199.45	-3.67	0.55	A190	220.51	-4.59	-1.53
107	183.61	-4.66	-0.66	164	201.31	-3.99	0.69	B190	220.74	-4.40	-1.32
108	183.97	-4.19	-0.47	165	201.99	-3.63	0.52	C190	220.90	-4.42	-1.38
109	184.17	-4.38	-0.61	166	202.15	-4.21	0.54	191	221.01	-3.99	-1.28
110	184.43	-4.59	-0.79	167	202.50	-4.03	0.58	A191	221.18	-4.64	-1.33
111	184.72	-4.51	-0.84	168	203.73	-4.78	0.52	B191	221.33	-4.37	-1.30
112	184.80	-4.89	-0.97		205.20	-5.14	0.58	C191	221.37	-4.34	-1.30
113	184.96	-3.87	-0.94		205.40	-5.51	0.55	D191	221.54	-4.84	-1.33
114	185.26	-3.89	-1.05		205.55	-5.04	0.51	E191	221.80	-5.33	-1.28
115	185.30	-3.98	-1.05		205.60	-4.85	0.63	F191	222.04	-5.03	-1.15
116	185.51	-4.31	-0.97	169	205.63	-4.78	0.63	192	222.08	-5.12	-1.14
118	185.65	-3.55	-1.08		205.80	-5.00	0.62	A192	222.14	-4.05	-1.30
118b	185.8	-5.45	-1.12		205.95	-4.69	0.59	193	222.20	-4.98	-1.01
119	185.96	-4.28	-0.89		206.10	-4.71	0.69	A193	222.27	-4.31	-1.10
120	186.15	-4.19	-0.83		206.20	-4.85	0.69	194	222.35	-4.26	-0.75
121	186.47	-4.65	-0.79		206.40	-4.71	0.58	A194	222.46	-4.29	-0.84
122	186.77	-4.68	-0.68		206.50	-4.09	0.46	B194	222.64	-4.18	-0.87
123	186.80	-4.55	-0.55		206.70	-4.40	0.54	C194	223.02	-4.44	-0.57
124	186.85	-5.53	-0.58	170	206.89	-4.43	0.58	D194	223.33	-4.50	-0.77
125	186.93	-4.69	-0.44		206.95	-3.93	0.61	E194	223.71	-4.11	-1.11
126a	186.97	-5.13	-0.45	171	207.14	-7.21	0.26	195	223.94	-4.10	-0.88
126b	187.05	-5.66	-0.88		207.30	-6.32	0.24	A195	224.04	-4.37	-0.98
127	187.20	-4.90	-0.27		207.50	-5.90	0.36	B195	224.37	-4.70	-0.77
128	187.45	-4.82	-0.31		207.75	-4.05	0.61	196	224.52	-5.18	-0.40
129	187.55	-4.85	-0.25		207.95	-2.94	-0.08	A196	224.73	-4.42	0.01
130	187.83	-4.67	-0.18		208.20	-3.84	0.27	B196	225.01	-4.38	0.33
131	188.15	-6.60	-0.27		208.30	-4.45	0.23	C196	225.22	-4.95	0.47
132	188.44	-4.56	-0.02		208.50	-4.43	0.54	197	225.40	-4.35	0.65
133	188.52	-4.59	0.01		208.75	-5.80	0.43	A197	225.64	-4.58	0.68
134	188.98	-4.63	0.38		209.20	-5.23	0.45	B197	225.84	-4.41	0.76
135	189.23	-4.44	0.48		209.30	-5.03	0.41	198	226.00	-4.25	0.81

Table 1 (continued).

Sample No.	Depth [m]	$\delta^{18}O$	$\delta^{13}C$
B198	226.12	-4.46	0.92
C198	227.02	-4.52	1.08
199	227.46	-4.44	1.25
A199	227.77	-4.59	1.28
B199	228.04	-4.49	1.33
C199	228.53	-4.38	1.26
D199	228.63	-4.39	1.16
200	228.94	-4.17	1.21
201	229.12	-4.06	1.22
A201	229.74	-4.80	1.14
202	229.65	-3.98	0.99
A202	229.74	-4.39	1.04
203	229.80	-5.74	1.10
204	229.92	-4.42	1.10
A204	230.03	-4.28	1.16
B204	230.46	-4.47	1.38
C204	230.60	-4.63	1.43
205	230.95	-6.00	1.43
206	231.25	-4.82	1.51
207	231.37	-4.77	1.54
208	231.72	-4.79	1.62
209	233.06	-3.36	1.54
210	233.60	-3.68	1.16
211	235.25	-2.67	1.74
212	235.77	-2.89	1.64
213	236.65	-3.51	1.79
214	236.76	-3.84	1.72
215	237.84	-3.33	2.08
216	240.26	-2.80	1.92
217	240.90	-4.18	1.98
218	241.89	-3.85	2.07
219	243.17	-2.33	1.86
220	243.60	-3.11	1.68
221	244.28	-2.80	1.75
222	247.95	-3.82	1.97
223	251.00	-2.04	2.27
	251.20	-3.06	1.99
	251.40	-2.68	2.10
	251.60	-3.86	2.10
	251.75	-2.43	2.27
224	251.85	-0.74	2.69
225	252.36	-3.27	2.12
	251.95	-1.57	2.05
	252.10	-1.82	2.04
	252.30	-2.38	2.03
	252.70	-1.58	2.42
	252.95	-1.12	2.43
	253.00	-2.37	2.50
	253.20	-1.40	2.50
	253.55	-1.38	2.42
	253.75	-2.64	2.30
	253.95	-1.81	2.40
	254.15	-3.24	2.23
226	254.28	-1.72	2.36
227	255.65	-1.37	2.29
228	256.54	-0.64	2.56
229	256.97	-1.93	2.55
230	257.35	-0.57	2.14
231	259.17	-0.76	2.50
232	259.50	-1.17	2.32
233	261.05	-1.80	2.46
234	261.83	-1.80	2.38
235	263.25	-1.33	2.45
236	263.54	-0.61	2.41
237	265.13	-1.81	2.41
238	266.80	-0.49	2.83
239	267.46	-0.58	2.66
240	269.75	-0.81	2.13
241	270.15	-0.20	2.03
242	270.80	-0.63	2.05
243	271.20	0.40	2.05
244	272.95	-1.04	2.15
245	273.85	-1.12	2.34
247	277.98	0.35	2.52
248	278.75	-0.68	2.44
249	279.67	-0.13	2.51
250	280.44	-1.12	2.51
251	281.45	-1.02	2.62
252	282.45	-0.94	2.66
253	282.71	-1.33	2.69
254	285.05	-0.89	2.83
255	286.33	-1.73	2.74
256	287.83	-0.24	2.85
257	289.07	-0.60	2.76
258	289.62	-1.18	2.33
259	290.37	-0.96	2.65
260	291.15	-0.94	2.85
261	291.26	-0.94	2.58
262	292.30	-0.36	2.68
263	292.60	-0.10	2.74
264	293.46	-0.48	2.98
265	294.80	0.29	3.05
266	295.29	-0.61	2.98
267	295.95	-0.45	3.32
268	296.40	-1.09	3.32
269	297.77	-0.55	3.51
270	298.05	0.08	3.52
271	299.60	0.06	3.29
272	299.92	-0.95	3.08
273	301.10	-1.65	2.94
274	303.15	-2.92	2.73
275	305.80	-0.69	2.95
276	306.80	-2.75	2.83
277	307.55	-0.63	3.13
279	310.02	-2.21	3.02
280	311.34	-0.11	3.19
281	312.10	0.00	3.24
282	313.58	-0.35	3.22
	313.65	-1.05	3.08
	313.75	-1.19	3.14
	313.85	-0.00	3.20
	313.95	-0.18	3.41
	314.05	-0.81	3.14
	314.15	-1.30	3.02
	314.20	0.57	3.24
	314.40	-1.25	2.94
	314.50	-1.88	2.85
	314.64	-0.63	3.01
	314.70	-1.14	2.91
	314.80	-0.79	2.78
284	314.85	-3.93	2.55
287	315.76	-2.42	2.87
288	317.05	-2.11	2.60
289	317.53	-2.76	2.71
290	318.50	-1.69	2.76
291	318.87	-3.16	2.66
292	321.43	-1.94	2.77
293	322.60	-2.38	2.64
294	322.90	-2.81	2.55
295	323.70	-3.68	2.61
296	324.80	0.33	3.18
297	326.55	-2.27	2.84
298	327.31	-3.05	2.66
299	328.06	-2.73	2.71
300	329.04	-0.41	3.04
301	330.00	-0.08	3.28

Table 2.
Oxygen and carbon isotope analyses of carbonates from the outcrop section Reppwand B.

Sample No.	Cumulative thickness at base [m]	$\delta^{18}O$ [‰ (PDB)]	$\delta^{13}C$ [‰ (PDB)]	Remarks*)
90	59.7	−6.25	0.97	
89	58.7	−5.11	1.03	
88	57.7	−5.05	0.99	
87	56.7	−4.83	0.85	
86	56.0	−4.77	0.91	
85	55.5	−4.74	0.85	
84	54.4	−4.65	0.78	
83	53.4	−4.46	1.03	
82	52.6	−3.92	0.94	
81	51.8	−3.60	0.82	
80	50.6	−4.27	0.70	
79	49.6	−3.60	0.62	
78	48.6	−3.76	0.22	
77	47.6	−3.84	−0.50	
76	46.6	−4.04	−0.46	
75	45.6	−4.20	−0.79	
74	44.7	−4.70	−1.15	Upper minimum $\delta^{13}C$ – correlates to 185.8 m in GK-1
73	43.4	−4.26	−0.96	
72	42.4	−4.36	−0.82	
71	41.4	−4.04	−0.43	
70	40.6	−3.89	0.00	
69	39.4	−4.11	0.22	
68	38.2	−4.69	0.60	
67	37.2	−3.71	0.81	Correlates to 189.2 m in GK-1
66	35.7	−3.26	0.65	
65	34.2	−4.27	0.20	
64	32.7	−4.73	−0.65	Middle minimum $\delta^{13}C$ – correlates to 193.0 m in GK-1
63	31.2	−4.43	−0.27	
62	29.7	−4.53	−0.45	
61	28.2	−4.37	0.43	
60	26.7	−4.27	0.20	
59	25.2	−3.96	0.47	
58	23.7	−5.33	0.94	
57	22.2	−5.14	0.61	
56	20.7	−5.22	0.47	
55	19.2	−5.17	0.80	
54	17.7	−4.34	0.38	
53	16.2	−5.13	0.33	
52	14.7	−4.52	0.30	
51	13.2	−5.22	−0.15	
50	11.7	−4.76	−0.53	
49	10.2	−4.37	−0.09	
48	8.1	−4.64	−0.28	
47	8.2	−5.3	−0.46	
46	8.2	−7.3	−0.50	
45	8.0	−5.5	−0.60	
44	7.8	−6.9	−1.01	
43	7.0	−6.3	−1.10	
42	6.9	−6.5	−1.27	
41	6.7	−6.8	−1.38	Lower minimum $\delta^{13}C$
40	6.5	−6.9	−1.00	
—	6.3	—	—	0.2 m dark gray dolomitic marl
38	5.8	−4.9	−0.99	
37	5.5	−5.5	−1.08	
86434	5.1	—	—	0.4 m homogeneous brown marl
86462	5.1	—	—	0.02 m brown shale
36	4.8	−5.9	−0.78	
36A	4.8	−5.6	−0.19	
35	4.6	−5.3	−0.28	
34	4.5	−5.4	−0.28	
33	4.5	−5.3	−0.18	
32	4.4	−5.1	−0.22	0.13 m dolomite, in part laminated
86460	4.4	—	—	0.001 m dark gray clay
30,86459	4.2	−5.1	0.24	0.2 m thinly platy gray marly dolomite
86458	4.2	—	—	0.003 m brown lamellar clay; 220 ppT Ir
29	4.1	−5.3	0.46	0.05 m gray lamellar dolomite
28,86456	4.0	−5.2	0.80	0.13 m gray lamellar dolomite
86455	4.0	—	—	0.001 m brown marl; 100 ppT Ir
27,86457	3.7	−5.5	1.15	
26	3.5	−5.5	1.40	
24	3.0	−4.6	−0.93	
23	2.8	−5.5	1.42	
22	2.5	−5.7	1.44	
20	2.0	−5.6	1.50	
18	1.3	−5.7	1.37	
17	0.9	−5.3	1.16	
14	0.4	−5.6	1.11	Correlates to 229.7 m in GK-1
13	0.2	−6.0	1.11	
12	0.0	−6.9	1.14	0.17 m brown marly dolomite
86450	0.0	—	—	0.02 m brown marly dolomite; Bellerophon/Werfen boundary
11	− 0.3	−6.3	1.54	
10	− 0.6	−5.4	1.49	
9	− 0.9	−5.3	1.47	
8	− 1.2	−5.5	1.40	
7	− 1.7	−4.8	1.27	
6	− 2.0	−5.2	1.40	
5	− 2.4	−5.1	1.72	
4	− 3.1	−4.3	1.42	
3	− 3.7	−3.7	1.51	

*) For conodont zonation see SCHÖNLAUB (this volume, Text-Fig. 3 and Table 2); for INAA analyses see ATTREP et al. (this volume, Table 17).

3.1. Unit 1A (293.46–330 m) – Bellerophon Formation

The carbon isotope composition of the carbonate rocks of this unit ranges from +2.5 to +3.5 ‰ (Text-Fig. 3), and is similar to other values reported from the Bellerophon Formation (W.T. HOLSER & M. MAGARITZ, 1985; M. MAGARITZ et al., 1988). Within this segment $\delta^{13}C$ values oscillated between low and high values. A detailed sampling of one of these oscillations (the zone of increasing $\delta^{13}C$ at 314 m) shows that the shift occurred within a 0.5 m section. $\delta^{18}O$ values in this unit show much larger variations, form −4.0 to +0.5 ‰ (Text-Fig. 3). The fluctuations of $\delta^{18}O$ are very similar to those of $\delta^{13}C$; thus a good correlation exists between the isotope values: $|r|$ for 46 samples is 0.84 (significance level better than 0.0001) (Text-Fig. 4). The detailed segment analyzed at 314 m shows that the $\delta^{18}O$ shift occurs within 10 cm and that it leads the $\delta^{13}C$ shift by 10 cm. These sharp changes in both the $\delta^{13}C$ and $\delta^{18}O$ records suggest that both isotope records have been substantially preserved. The preservation of the carbon isotope record is common in carbonate rocks (M. MAGARITZ, 1983), but preservation of the oxygen record would require an unusual lack of water circulation through the section.

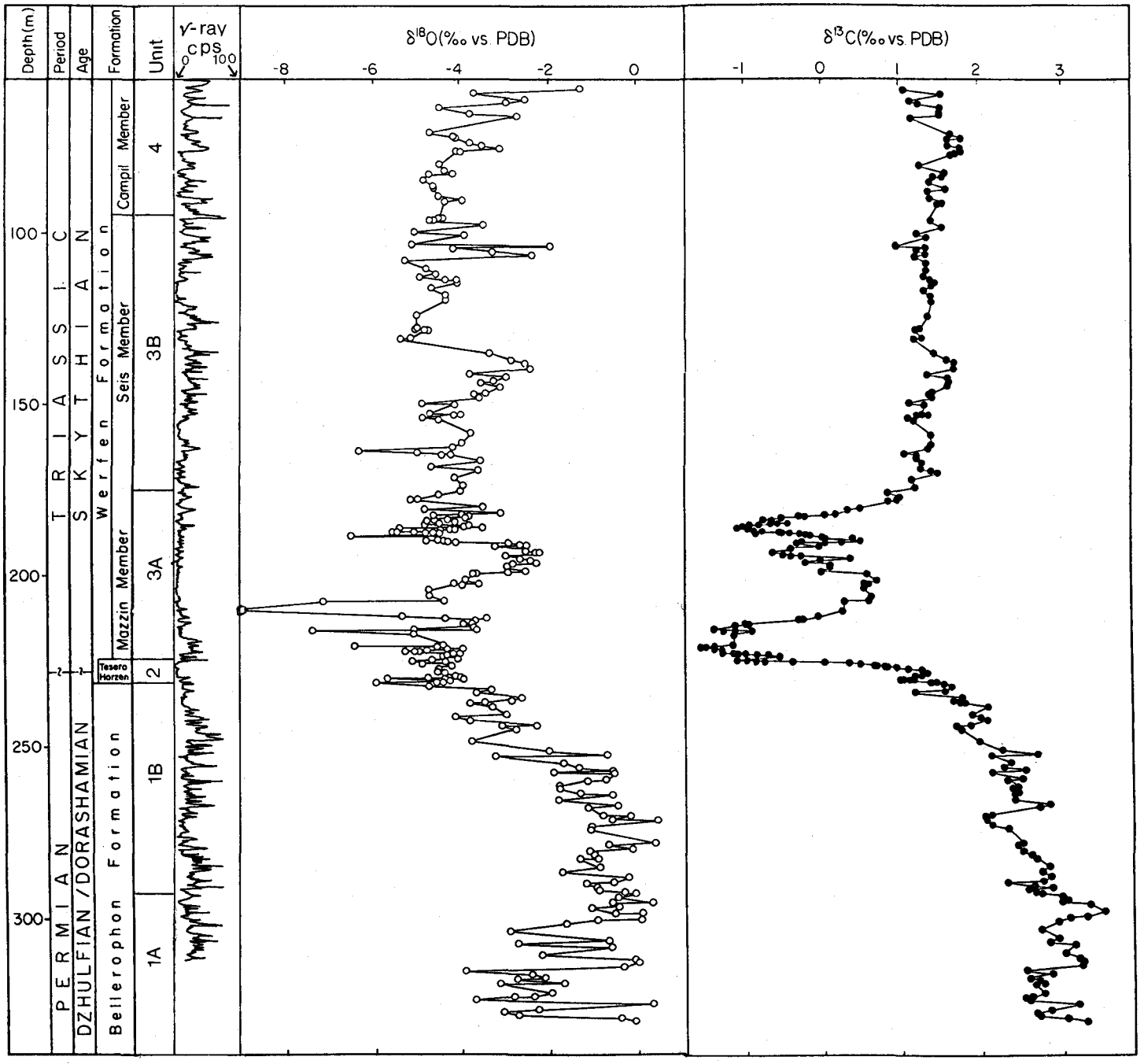

Text-Fig. 2.
Oxygen and carbon isotope composition in carbonate rocks across the Permian/Triassic boundary in the Gartnerkofel-1 core.
Specific aspects of each of 7 subunits are discussed in the text and illustrated in Text-Figs. 3–13. In this and the following Text-Figs. 3–13 the filled symbols are shaly samples.

3.2. Unit 1B (230.60–293.4 m) – Bellerophon Formation

Carbon isotopes in this unit show a gradual decrease from the base (about +2.8 ‰) to the top of the Bellerophon Formation (+1.5 ‰). The $\delta^{13}C$ values (Text-Fig. 5) drop in two segments, separated by a sharp rise between 270 and 266.8 m. The first drop of 0.8 ‰ in $\delta^{13}C$ values takes places smoothly between 282 and 270 m. After a sharp return a second drop, in the interval 267 to 231 m, is at a rate of −0.5 ‰/10 m, the slowest rate of decrease in the whole overlying profile (Table 2). Comparing the Gartnerkofel section to the Tesero section 140 km to the west the change in $\delta^{13}C$ from +3 ‰ to +1.5 ‰ occurs at Tesero between two samples (lines A and B, Text-Fig. 1 in M. MAGARITZ et al., 1988), so most of the equivalent section may be missing there.

The $\delta^{18}O$ values in this section show two groups at different depths: the lower part (about −1 ‰) from 293 to 254 m; and the upper part with values around −3 ‰ (Text-Fig. 5). No change of $\delta^{18}O$ is found corresponding to the first drop of $\delta^{13}C$ (282 to 270 m). A detailed sampling at the transition zone between the two groups of $\delta^{18}O$ values show adjacent samples with both ^{18}O enriched and ^{18}O depleted. The first sample

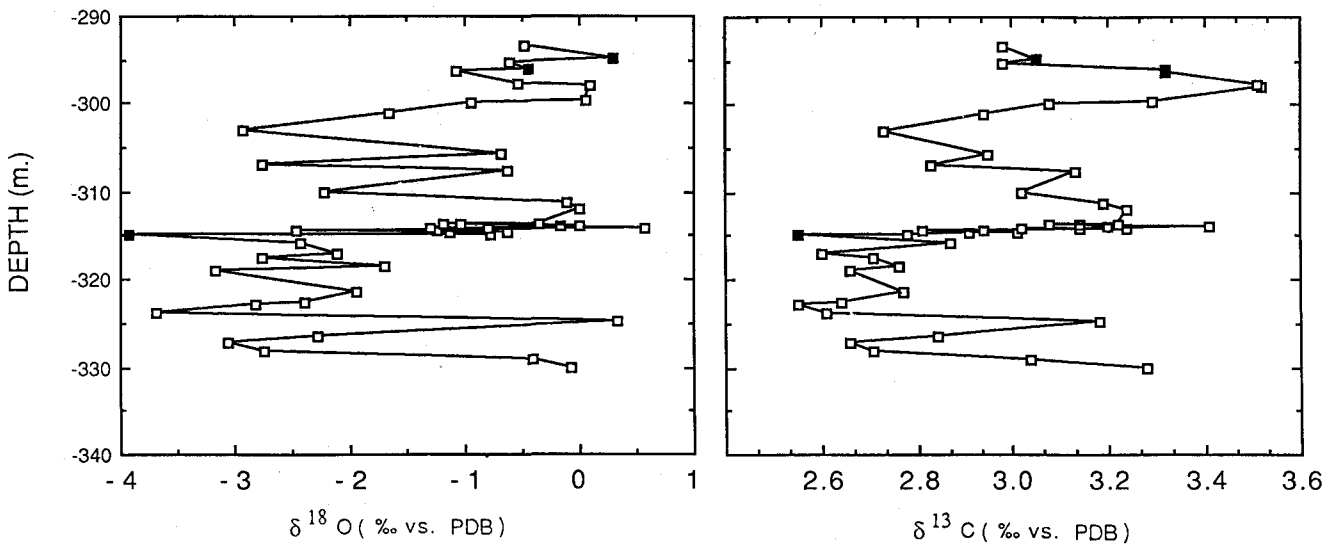

Text-Fig. 3.
Oxygen and carbon isotope variations in Unit 1A (293.46–330 m) of the Permian Bellerophon Formation.
In this segment $\delta^{13}C$ is generally high, but both isotopes oscillate between higher and lower values.

depleted in ^{18}O is found at 254.15 m and the last ^{18}O enriched sample at 251.85 m.

$\delta^{18}O$ and $\delta^{13}C$ are correlated (r = 0.74, significance level 0.0001) over the whole unit (Text-Fig. 6), but most of that correlation is owing to their bimodal groupings in depth. Thus most of the samples depleted in ^{18}O (<2 ‰) have $\delta^{13}C$ <2.3 ‰, but are also at a depth of less than 254 m.

3.3. Unit 2 (230.95–224.7 m) – The Tesero Horizon

In the lower part of this unit a drop of 0.5 ‰ in $\delta^{13}C$ is followed by an increase to almost the same level, and then by the fastest shift in $\delta^{13}C$ values (–4.0 ‰/10 m, Text-Fig. 7, Table 3). The thickness of the Tesero Horizon in this section is similar to that at Tesero (M. MAGARITZ et al., 1988), and the magnitude of the $\delta^{13}C$ drop, of 1.5 ‰, is almost the same in the two sections.

$\delta^{18}O$ values drop to ≤–4 ‰ and remain constant in the unit (Text-Fig. 7), as in the section at Tesero. Exceptions are the two samples of marl, which are depleted in ^{18}O by a further 2 ‰ (Text-Fig. 7), but which also have high (42 and 85 %) insoluble residue (P. KLEIN, this volume). This depletion may indicate a late exchange of oxygen isotopes in the carbonate phase. It is important to note that whereas large shifts in $\delta^{18}O$ values are observed in these samples, no changes in $\delta^{13}C$ values were detected: the samples above and below the marl at 231 m have $\delta^{13}C$ values of +1.51 and +1.43 ‰, while the marl sample has a value of +1.43 ‰; the samples above and below the marl at 229.8 m have $\delta^{13}C$ values of +1.10 ‰, and 1.04 ‰, while the marl sample has a value of +1.10 ‰. It is possible that the marl layers are the channels where more fluid passed, thus affecting their $\delta^{18}O$ values, as is also detected by the slight depletion of $\delta^{18}O$ in the samples just above the marl beds (Text-Fig. 7).

Table 3.
Rates of changes in the carbon isotope ratio near the Permian/Triassic Boundary, Gartnerkofel-1 core.

Unit	Begin [m]	End [m]	Begin $\delta^{13}C$ [‰]	End $\delta^{13}C$ [‰]	Rate [‰/10 m]
3A-3 (Upper excursion)	185.30	176.32	–1.05	+0.97	+2.3
3A-3 (Upper excursion)	189.23	185.30	+0.48	–1.05	–3.9
3A-2 (Middle excursion)	193.00	189.23	–0.67	+0.48	+3.0
3A-2 (Middle excursion)	201.31	193.00	0.69	–0.67	–1.6
3A-1 (Lower excursion)	215.07	210.50	–1.41	0.42	+4.0
2+3A-1 (Lower excursion)	228.04	220.20	+1.33	–1.57	–3.7
3A-1 (Lower excursion)	224.52	220.20	–0.40	–1.57	–2.7
2	228.04	224.73	+1.33	+0.01	–4.0
1B	266.80	231.25	+2.83	+1.54	–0.5
Mean rate of $\delta^{13}C$ decrease					2.7±1.4
Mean rate of $\delta^{13}C$ increase					3.1±0.89

3.4. Unit 3A-1 (224.52–201.31 m) – The Lower Negative Excursion of $\delta^{13}C$ in the Mazzin Member

The carbon isotope values in this interval reach the first minimum at 220 m (Text-Fig. 8). This minimum represents the most depleted ^{13}C (–1.5 ‰) of the entire core section. In the lower part of this unit, coming into the minimum, the rate of decrease of $\delta^{13}C$ is only slightly lower (–2.7 ‰/100 m) than in the Tesero Horizon (Table 4). The $\delta^{13}C$ values rise at a very fast rate above 215.0 m (+4.0 ‰/100 m, Table 4), followed by a zone with almost constant $\delta^{13}C$ values (+0.5 ‰), from 210.5 m to the top of the unit.

In this segment of the core a major fault was evident at 207–211 m (K. BOECKELMANN, this volume), and this interval was characterized by the greatest ^{18}O depletion of the entire core (–6 to –9 ‰). Note again that the shift in $\delta^{18}O$ was not accompanied by a change in $\delta^{13}C$ values of the carbonate phase. The extent of the depletion of $\delta^{18}O$ values near the fault is seen by the large variability in nearby samples (Text-Fig. 8).

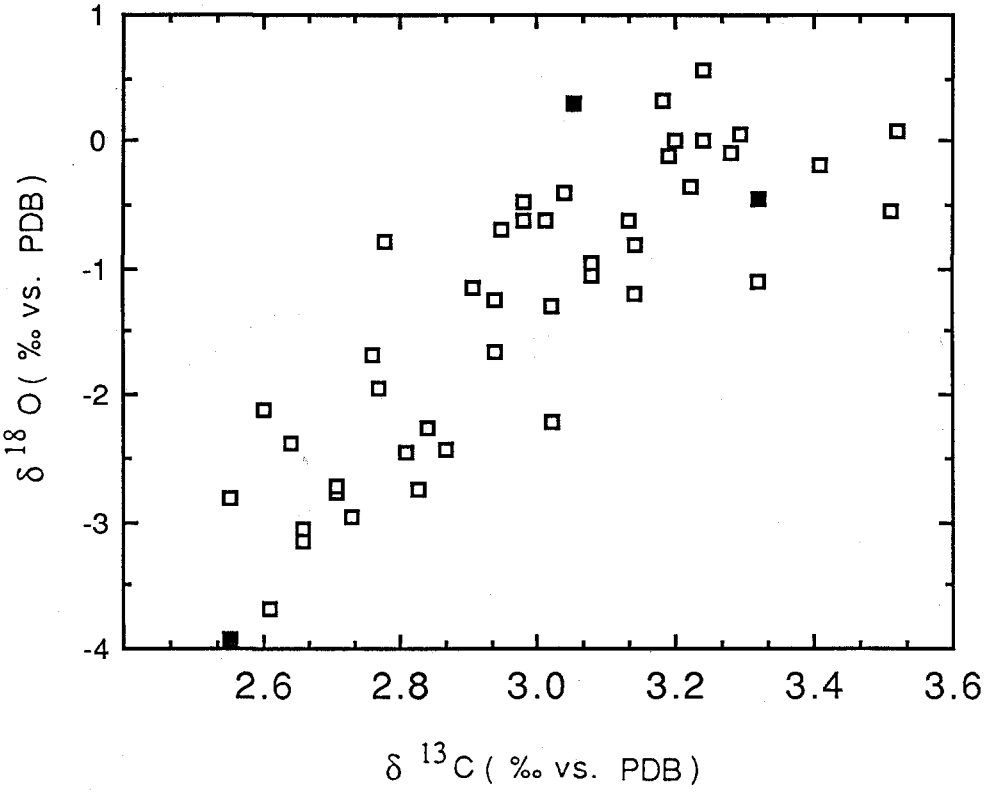

Text-Fig. 4.
Cross-plot of the variations in Unit 1A2 (Fig. 2) showing a significant correlation ($p<0.0001$) between $\delta^{18}O$ and $\delta^{13}C$.

3.5. Unit 3A-2 (199.45–189.65 m) – The Middle Negative Excursion of $\delta^{13}C$ in the Mazzin Member

The carbon isotope data for this unit show a depletion of $\delta^{13}C$ at a rate of −1.6 ‰/10 m (Table 3), and a subsequent enrichment with almost double the rate +3.0 ‰/10 m (Text-Fig. 4). $\delta^{83}O$ values in this unit are rather constant, and are the most enriched in ^{18}O of all the Triassic section analyzed (Text-Fig. 9); exceptions are the lowermost and uppermost samples which are depleted in ^{18}O by 1–2 ‰.

3.6. Unit 3A-3 (189.30–175.10 m) – The Upper Negative Excursion of $\delta^{13}C$ in the Mazzin Member

This excursion of $\delta^{13}C$ is almost symmetric, with rates of −3.9 ‰/10 m decrease (Text-Fig. 10) followed by +2.3 ‰/10 m increase (Text-Fig. 11). This segment of the core includes a relatively large number of marl and sulfide horizons (P. KLEIN, this volume), and as can be seen in Text-Figures 10 and 11 $\delta^{13}C$ of the marl samples are still those expected by interpolation from the carbonate samples below and above. $\delta^{18}O$ values show relatively high variability (Text-Figs. 10 and 11), mainly in the upper part of the unit. The carbonate in the marly horizons is mostly depleted in ^{18}O as in unit 2.

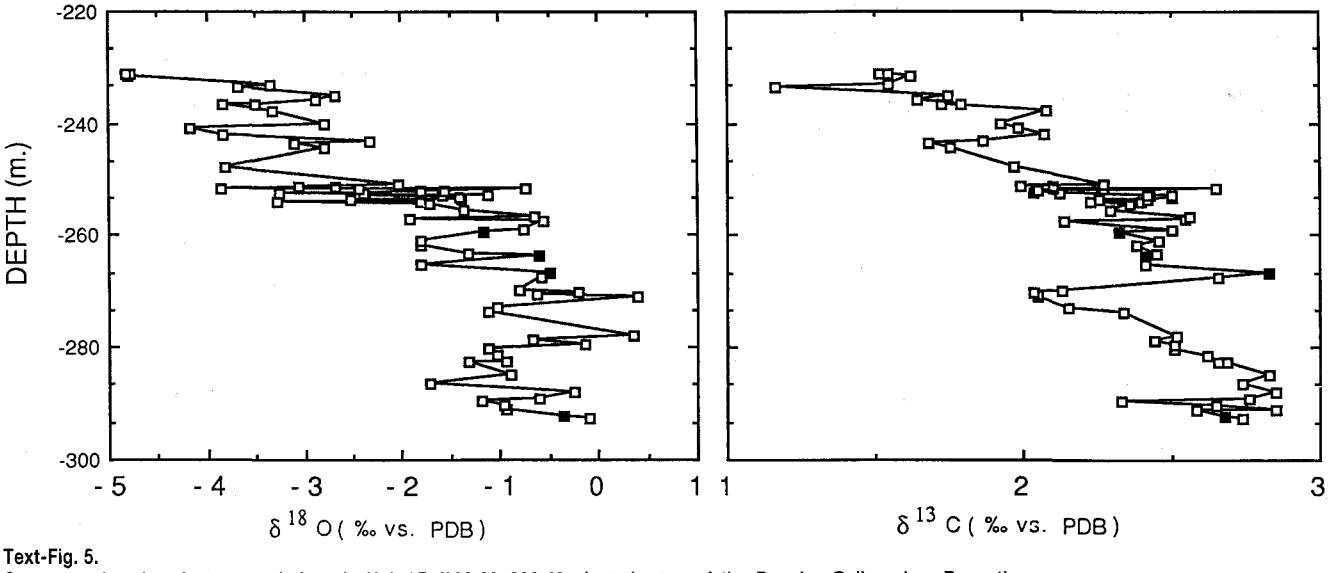

Text-Fig. 5.
Oxygen and carbon isotope variations in Unit 1B (230.60–293.40 m) at the top of the Permian Bellerophon Formation.
$\delta^{13}C$ drops steadily from 267 to 231 m, while $\delta^{18}O$ drops sharply around 252 to 254 m.

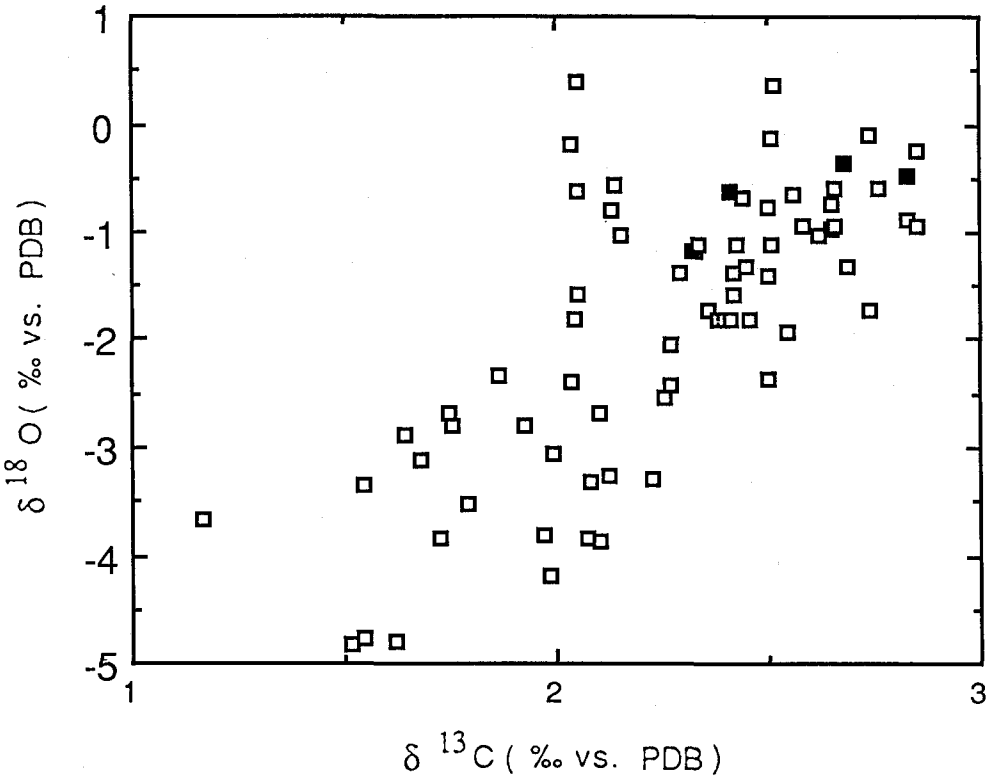

Text-Fig. 6.
Cross-plot of the variations in Unit 1B (Fig. 4).
Although the correlation is formally significant ($p<0.0001$), the correlation is mainly a consequence of the bimodal grouping of $\delta^{18}O$.

3.7. Unit 3B and 4 (173.52–57.53 m) – The Remainder of the Skythian Section

In the rest of the Triassic sequence the $\delta^{13}C$ values are rather constant (Text-Fig. 12), with minor variation between +1.0 and +1.7 ‰. Two zones slightly enriched in $\delta^{13}C$ are found around 70 and 140 m. The marl samples do not significantly differ in $\delta^{13}C$ from nearby carbonates.

$\delta^{18}O$ values (Text-Fig. 12) are relatively depleted in ^{18}O but rather constant (–4.5 ‰) with few samples enriched in ^{18}O. One of the zones of ^{18}O enrichment (≈140 m) is also enriched in ^{13}C.

3.8. The Reppwand Outcrop Section

In order to determine the local variability of the carbon isotope excursions, part of the section was also sampled on cliff outcrops of the Reppwand, 500 m northwest of Gartnerkofel-1. The data are listed in Table 2 and the carbon isotope data are plotted parallel to the equivalent section of the core in Text-Fig. 13. As can be seen, the general shape of the three minima is clearly reproduced, with almost the same distance between the minima: 25 m (lower to middle minima) and 10 m (middle to upper minima). The values of the minima on the outcrop section –1.38, –0.65 and

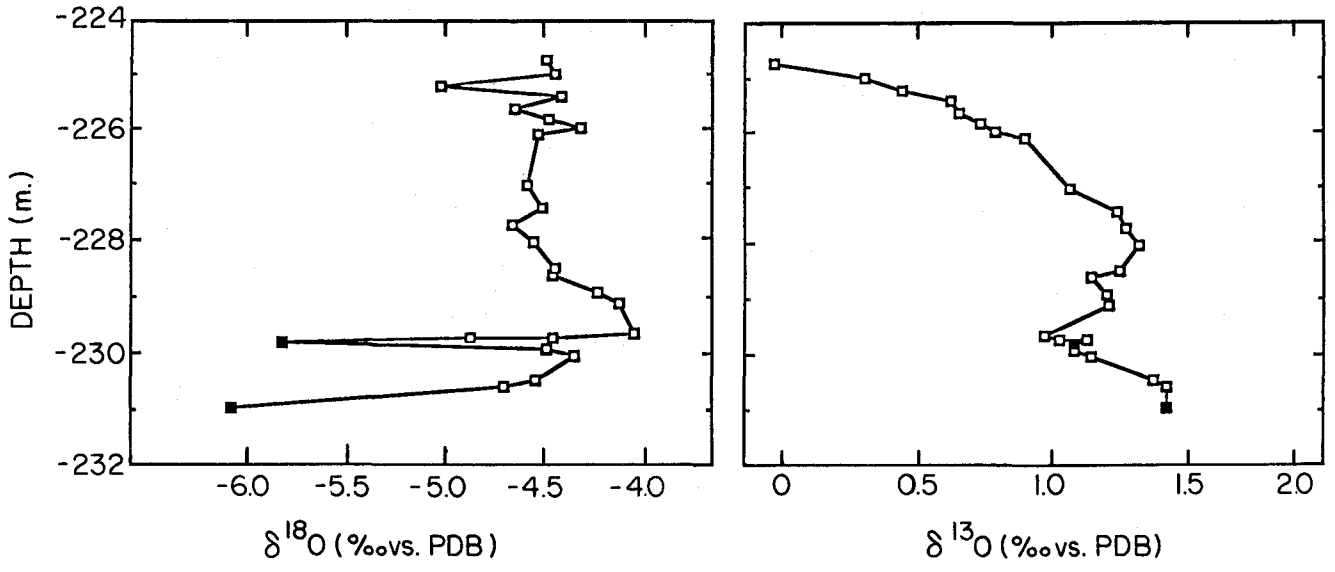

Text-Fig. 7.
Oxygen and carbon isotope variations in Unit 2 (231–225 m), the Tesero Horizon that includes the P/Tr boundary.
Essentially $\delta^{13}C$ drops smoothly and steeply through the P/Tr boundary, while ^{18}O remains constant (except the two marl samples have exchanged ^{18}O).

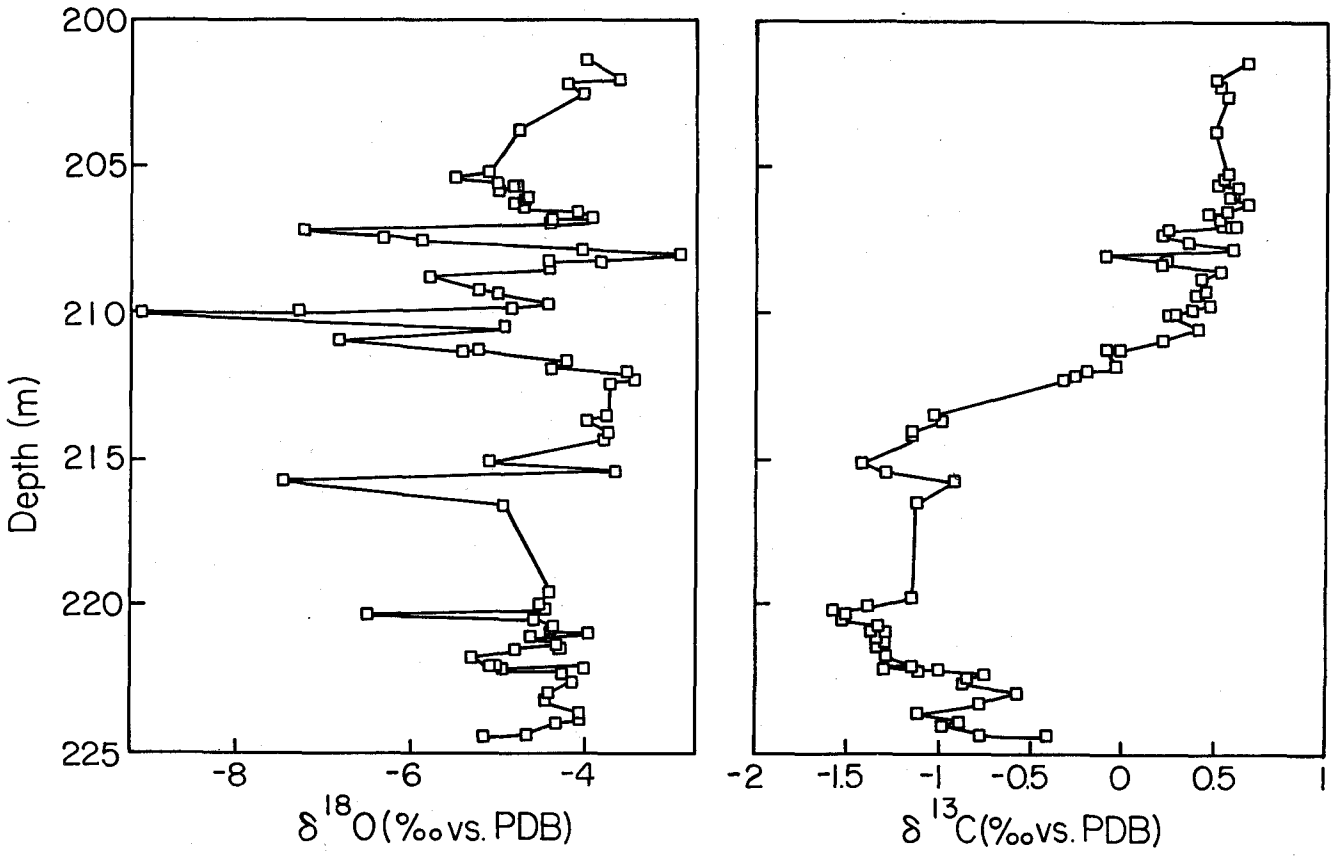

Text-Fig. 8.
Oxygen and carbon isotope variations through the lower negative excursion of $\delta^{13}C$ (Unit 3A-1, 225–201 m) at the base of the Mazzin Member of the Triassic Werfen Formation.
Faulting at 207–211 pulls down $\delta^{18}O$ without affecting the pattern of $\delta^{13}C$.

−1.15 ‰ are similar to those in the core section −1.57, −0.67 and −1.12 ‰, thus confirming both the shape and size of the carbon isotope excursions in this area.

4. Discussion

4.1. Oxygen Isotopes

The question of preservation of the oxygen isotope record in carbonate rocks has been long debated in the isotope literature. The fact that, in many marine carbonate formations, ^{18}O is depleted relative to the concentration expected for marine carbonate, led to the idea that exchange generally occurred between the solid carbonate phase and meteoric water. The question, in which stage of diagenesis the exchange took place, was not clear; in many cases it was shown to be associated with transformation of marine phases (aragonite and high Mg-calcite) to low Mg-calcite (M.G. GROSS, 1964; M. MAGARITZ et al., 1979). On the one hand it is clear from mass balance calculation of a diagenetic environment (mixture of sediments and

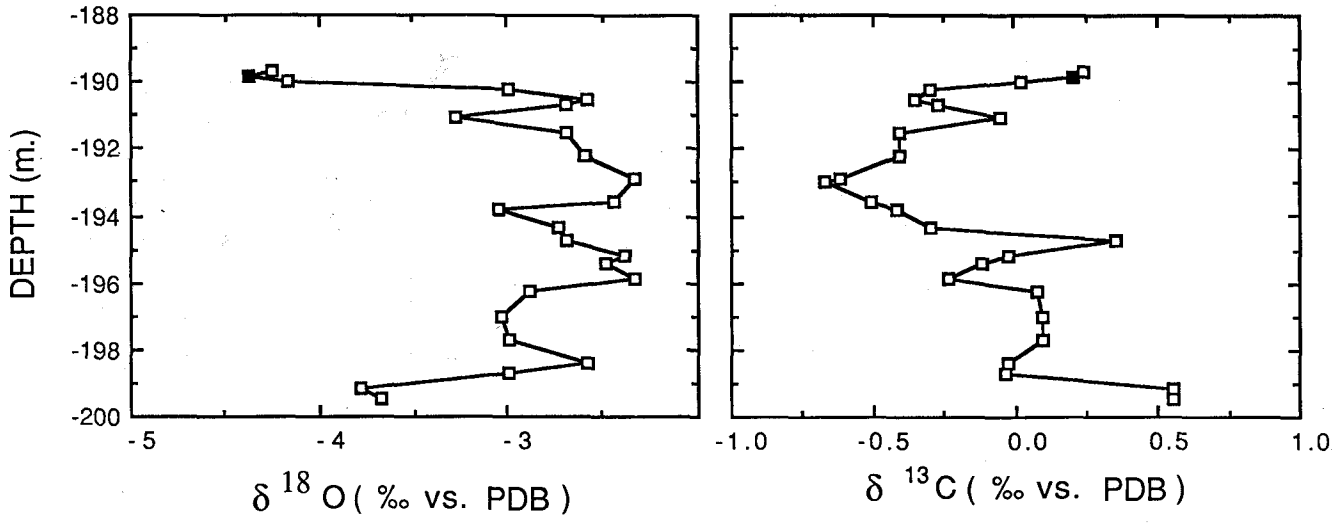

Text-Fig. 9.
Oxygen and carbon isotope variations through the middle negative excursion of $\delta^{13}C$ (Unit 3A-2, 189–175 m).

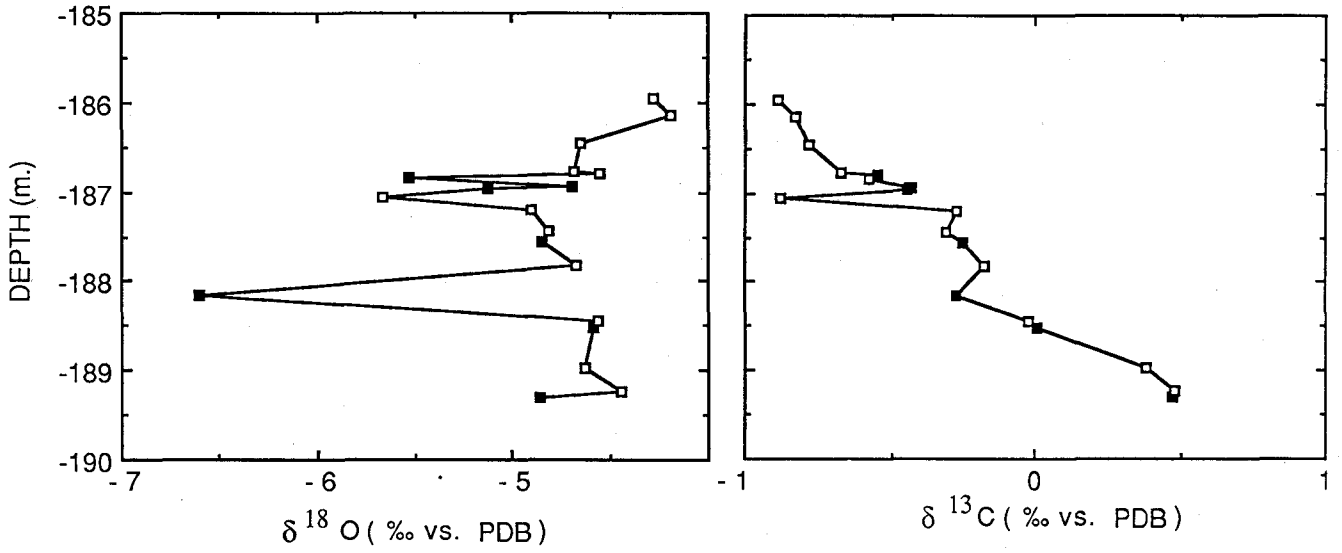

Text-Fig. 10.
Oxygen and carbon isotope variations through the approach to the upper negative excursion of $\delta^{13}C$ (Unit 3A-3, 189–175 m) in the Mazzin Member of the Triassic Werfen Formation.

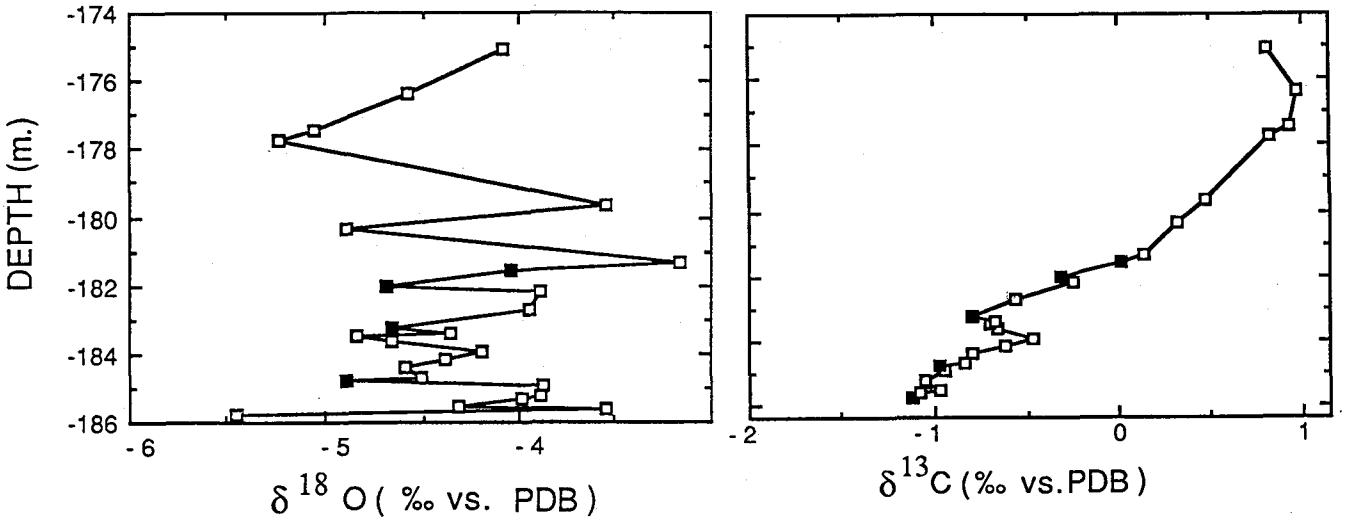

Text-Fig. 11.
Oxygen and carbon isotope variations through recovery from the upper negative excursion of $\delta^{13}C$ (Unit 3A-3).

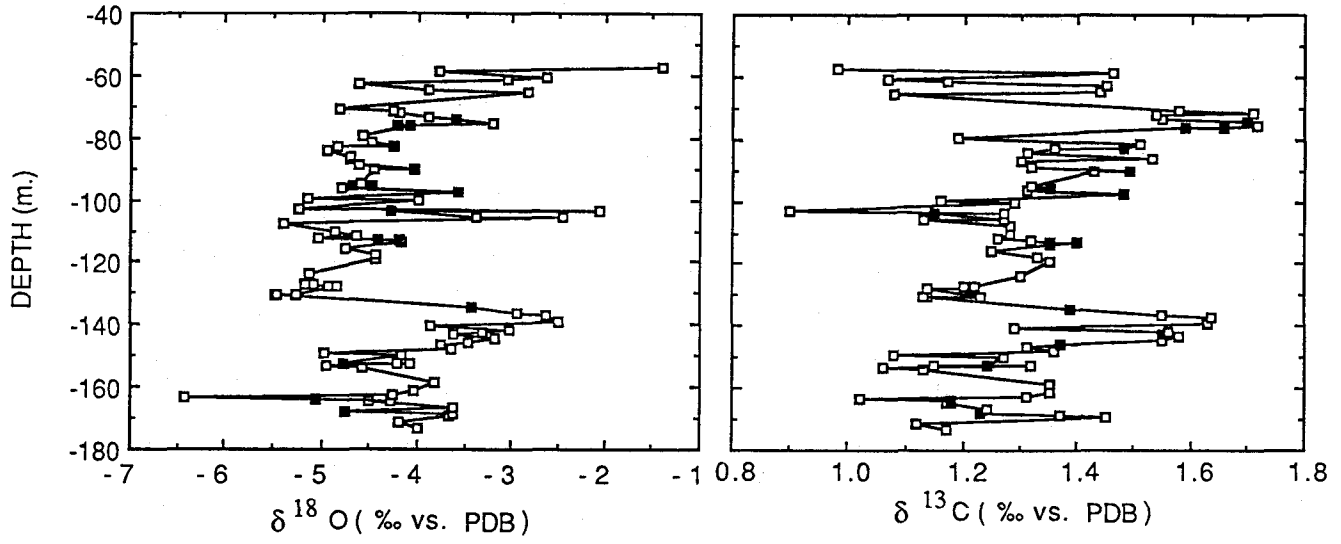

Text-Fig. 12.
Oxygen and carbon isotope compositions in the top part of the core, in Unit 3B and 4 (174–58 m) of the Mazzin and Seis Members of the Triassic Werfen Formation.

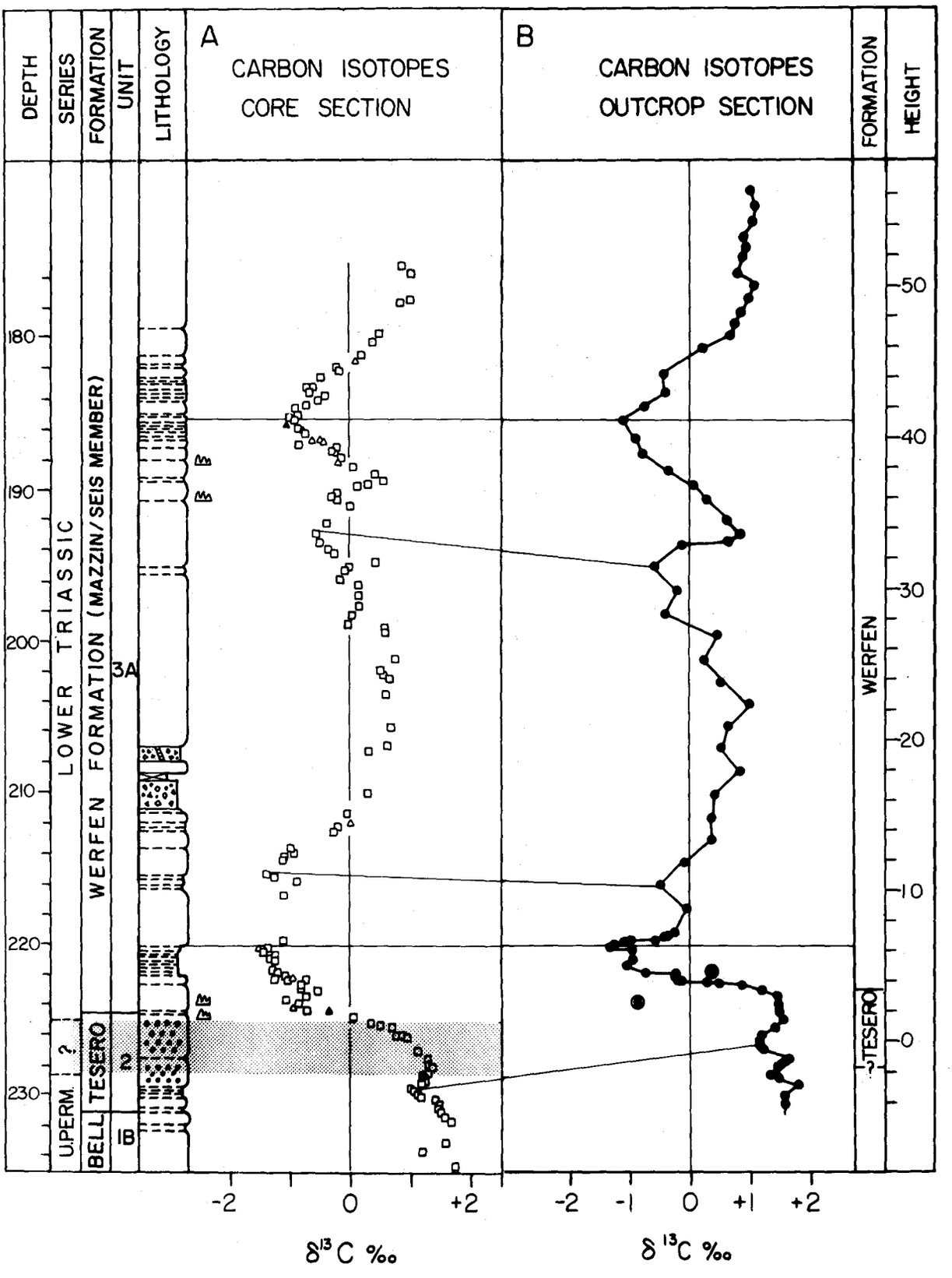

Text-Fig. 13.
Comparison of carbon isotope profiles in the Gartnerkofel-1 core and the Reppwand outcrop section approx. 500 m northwest.
The scale for the outcrop sections begins with an arbitrary zero at the Bellerophon-Werfen (*Tesero Horizon*) boundary. Correlation lines relate correlative features of the two carbon isotope profiles. These correlations are consistent with the detailed discussions of paleontology (H.P. SCHÖNLAUB, this volume; C. JENNY-DESHUSSES, this volume) and microfacies (K. BOECKELMANN, this volume). The Permian/Triassic boundary is close to the base of the Tesero Horizon as indicated by conodonts (H.P. SCHÖNLAUB, this volume). In the core section the samples in which peaks of iridium were determined (M. ATTREP JR. et al., this volume) are shown as filled triangles.

water) that the oxygen isotope ratio of the water should control that of the system (M. MAGARITZ, 1983). On the other hand, in systems with very low permeabilities like chalk and marls the oxygen isotope record may be preserved in samples that do not have substantial added cement (M. MAGARITZ, 1974; N.O. JØRGENSEN, 1987).

The oxygen isotope data presented in this study suggest that some of the original isotope record is preserved here. Though this cannot be proven, the pattern of the oxygen isotopes suggests that primary variations are observed. Primary features appear in both large- and fine-scale records. The large scale variation is represented by the general change in $\delta^{18}O$ values from the Bellerophon to Werfen Formations (Text-Fig. 2). The $\delta^{18}O$ values in the Bellerophon Formation varied between 0.5 to −3 ‰, and change in the upper Bellerophon transition zone to values in the range of −2.5 to −5 ‰ in the Werfen Formation. The transition between the two groups of values is sharp, occurring within a few meters in Unit 1B (Text-Fig. 5); the overall shift was about −3 ‰. Note that similar differences in the oxygen isotope record are found also in the section at Tesero between these two formations (M. MAGARITZ et al., 1988). Preservation of microfacies (K. BOECKELMANN, this volume) and of finely disseminated intergrain diagenetic pyrite in most of the sequence (K. BOECKELMANN & M. MAGARITZ, this volume), both support the suggestion that the amount of late fluids passed through the sequence was relatively small.

The rock has never been subjected to post-depositional thermal alteration, attested by the low grades of illite crystallinity (J.-M. SCHRAMM, this volume) and conodont alteration index (H.P. SCHÖNLAUB, this volume).

To the extent that the variations of $\delta^{18}O$ are primary and reflect ocean water conditions, they may have been caused by a change of temperature of deposition, or by a change in $\delta^{18}O$ of the water, or some combination of the two. To explain the overall shift of −3 ‰ by temperature alone would require an increase of 11°C across the P/Tr boundary, which seems excessive. Alternatively the decrease of $\delta^{18}O$ could be ascribed to a decrease of salinity. Under various marine conditions, $\delta^{18}O$ of evaporating sea water can rise a maximum of +6 ‰ as its concentration approaches 3.5 × sea water and the inception of gypsum precipitation (R.M. LLOYD, 1966). Evaporite deposition is common in the Bellerophon Basin especially a hundred kilometers or more west of Gartnerkofel, where it occurs both in the Permian Bellerophon Formation and in the Triassic Werfen Formations (R. ASSERETO et al., 1973; A. BOSSELLINI & L.A. HARDIE, 1973). At the Gartnerkofel traces of evaporites ("Rauhwacken") are found near the base of the Bellerophon Formation (W. BUGGISCH, 1974), tens of meters below the level reached in the core, and there does not seem to be any sedimentological break indicative of a salinity change near the Bellerophon/Werfen boundary. The cause of the large shift in $\delta^{18}O$ near the P/Tr boundary, and indeed the question as to whether it is really primary, remains open.

The samples most depleted in ^{18}O in the whole core are found at depth 210 m associated with a fault zone. Several nearby samples also show depletion in ^{18}O relative to the rest of the sequence (Text-Fig. 8). This indicates exchange with ^{18}O-depleted water; as the results show, this depletion is very limited spatially.

4.2. Carbon Isotopes

The carbon isotope data in this area persents the best record of carbon isotope changes across the P/Tr boundary. The continuity of deposition and the long record of biozonation in the Griesbachian Stage (the first stage of the Lower Triassic) are firmly established for this section by H.P. SCHÖNLAUB (this volume). Most of the classical sections studied elsewhere in Tethys by BAUD et al. (1989) do not show the complex features found in this section. Generally the overall drop to low values of $\delta^{13}C$ can be recognized. In most of the cases the drop occurred very sharply (within a few meters) without the long transition zone seen in unit 1B. Even in sections from the Alps west to this area (M. MAGARITZ et al., 1988) this important part of the sequence is missing. The extended minima zone of ^{13}C was also noted in other sections at Kuh-e-Ali Bashi (northwestern Iran) and Emarat (Northern Iran) (BAUD et al., 1989). But in neither of these localities were the clear details with three minima detected.

The drop in $\delta^{13}C$ values reflects changes in the carbon cycle, a shift from a reduced phase (organic carbon) to an oxidized phase (dissolved carbonate) (W.T. HOLSER & M. MAGARITZ, 1987). The gradual ^{13}C depletion at the Upper Permian (Unit 1) may reflect oxidation of organic matter associated with the continuous drop in sea level during the last few million years of the Permian (W. T. HOLSER & M. MAGARITZ, 1987). The shape of the carbon isotope curve suggests that at least three separate phases of oxidation of organic matter occurred, possibly corresponding to stages in lowering of sea level. At least some of the organic carbon probably derived from paralic coal beds, consequently, the three minima of ^{13}C may reflect phases of subaerial erosion elsewhere. Apparently this process ended with unit 3B, and $\delta^{13}C$ values remain almost constant during the rest of the Lower Triassic.

Acknowledgement

We would like to thank Mrs. R. SILANIKOV for stable isotope measurements.

References

ASSERETO, R., BOSSELINI, A., FANTINI SESTINI, N. & SWEET, W.C.: The Permian-Triassic Boundary in the Southern Alps (Italy). – Can. Soc. Petrol. Geol. Mem., **2**, 176–199, Calgary 1963.

BAUD, A., MAGARITZ, M. & HOLSER, W.T.: Permian-Triassic of Tethys: Carbon Isotope Studies. – Geol. Rdsch., **78**, 649–677, Stuttgart 1989.

BOSSELINI, A. & HARDIE, L.A.: Depositional Theme of a Marginal Marine Evaporite. – Sedimentology, **20**, 5–27, Amsterdam 1973.

BUGGISCH, W.: Die Bellerophonschichten der Reppwand (Gartnerkofel) (Oberperm, Karnischen Alpen). – Carinthia, **164**, 17–26, Kagenfurt 1974.

CLAYTON, R.N., SKINNER, H.C.W., BERNER, R.A. & ROBINSON, M.: Isotopic Composition of Recent Australian Lagoonal Carbonates. – Geochim. Cosmochim. Acta, **32**, 983–988, New York 1968.

GROSS, M.G.: Variations in the O^{18}/O^{16} and C^{13}/C^{12} Ratios of Diagenetically Altered Limestones in the Bermuda Islands. – J. Geol., **72**, 170–194, Chicago 1964.

HOLSER, W.T. & MAGARITZ, M.: The Late Permian Carbon Isotope Anomaly in the Bellerophon Basin, Carnic and Dolomite Alps. – Jb. Geol. B.-A., **128**, 75–82, Wien 1985.

HOLSER, W.T. & MAGARITZ, M.: Events Near the Permian-Triassic Boundary. – Mod. Geol., **11**, 155–180, 1987.

HOLSER, W.T., MAGARITZ, M. & CLARK, D. L.: Carbon Isotope Stratigraphic Correlations in the Late Permian. – Amer. J. Sci., **286**, 390–402, New Haven 1986a.

HOLSER, W.T., MAGARITZ, M. & WRIGHT, J.W.: Chemical and Isotopic Variations in the World Ocean During Phanerozoic Time. – In: WALLISER, O. (ed.): Global Bioevents, 63–74, Berlin (Springer-Verlag) 1986b.

JØRGENSEN, N.O.: Oxygen and Carbon Isotope Compositions of Upper Cretaceous Chalk from the Danish sub-Basin and the North Sea Central Graben. – Sedimentology, **34**, 599–570, Amsterdam 1987.

KAUFFMAN, E.G., ELDER, W.P. & PRATT, L.M.: Environmental and Biological Dynamics of the Cenomanian–Turonian Mass Extinction Event: Western Interior of North America. – In: Third International Conference on Global Bioevents: Abrupt Change in the Global Biota, Abstr. p. 22, University of Colorado (Boulder) 1988.

LLOYD, R.M.: Oxygen Isotope Enrichment of Sea Water by Evaporation. – Geochem. Cosmochim. Acta, **30**, 801–814, New York 1966.

MAGARITZ, M.: Lithification of Chalky Limestone: a Case Study of Senonian Rock from Israel. – J. Sedim. Petrol., **44**, 947–957, Tulsa 1974.

MAGARITZ, M.: Carbon and Oxygen Isotope Composition of Recent and Ancient Coated Grains. – In: PERYT, T.M. (ed.): Coated Grains, 27–37, Berlin (Springer Verlag) 1983.

MAGARITZ, M.: ^{13}C Minima Follow Extinction Events: A clue to Faunal Radiation. – Geology, **17**, 337–340, Boulder 1989.

MAGARITZ, M., GAVISH, E., BAKLER, N. & KAFRI, U.: Carbon and Oxygen Isotope Composition – Indicators of Cementation Environment in Recent, Holocene and Pleistocene Sediments along the Coast of Israel. – J. Sedim. Petrol., **49**, 401–412, Tulsa 1979.

MAGARITZ, M., BÄR, R., BAUD, A. & HOLSER, W.T.: The Carbon-Isotope Shift at the Permian/Triassic Boundary in the Southern Alps is Gradual. – Nature, **331**, 337–339, London 1988.

MAGARITZ, M., HOLSER, W.T. & KIRSCHVINK, J.L.: Carbon Isotope Events across the Precambrian/Cambrian Boundary on the Siberian Platform. – Nature, **320**, 258–259, London 1986.

MARGOLIS, S.V., MOUNT, J.F., DOEHNE, E., SHOWERS, W. & WARD, P.: The Cretaceous/Tertiary Boundary Carbon and Oxygen Isotope Stratigraphy, Diagenesis, and Paleoceanography at Zumaya, Spain. – Paleoceanography, **2**, 361–367, Washington 1987.

MCCREA, J.M.: The Isotopic Chemistry of Carbonates and Paleo-Temperature Scale. – J. Chem. Phys., **18**, 849–857, New York 1950.

ORTH, C.J., GILMORE, J.S., QUINTANA, L.R. & SHEENAN, P.M.: Terminal Ordovician Extinction: Geochemical analysis of the Ordovician/Silurian boundary, Anticosti Island, Quebec. – Geology, **14**, 433–436, Boulder 1986.

PLAYFORD, P.E., MCLAREN, D.J. ORTH, C.J., GILMORE, J.S. & GOODFELLOW, W.D.: Iridium Anomaly in the Upper Devonian of the Canning Basin, Western Australia. – Science, **226**, 437–439, Washington 1984.

POPP, B.N., ANDERSON, F.T. & SANDBERG, P.A.: Brachiopods as Indicators of Original Isotopic Composition in Paleozoic Limestones. – Geol. Soc. Amer. Bull, **97**, 1262–1269, Boulder 1986.

WALTERS, L.J., CLAYPOOL, G.E. & CHOQUETTE, P.M.: Reaction Rates and $\delta^{18}O$ Variation for the Carbonate-Phosphoric Acid Preparation Method. – Geochim. Cosmochim. Acta, **36**, 129–140, New York 1972.

XU, D.-Y., YAN, Z., ZHANG, Q.-W., SHEN, Z.-D., SUN, Y. A. and YE, L.-F.: Significance of a $\delta^{13}C$ Anomaly Near the Devonian/Carboniferous boundary at the Nuhua Section, South China. – Nature, **321**, 854–855, London 1986.